ChemComm

ROYAL SOCIETY OF CHEMISTRY

COMMUNICATION

View Article Online
View Journal | View Issue

Cite this: *Chem. Commun.*, 2020, **56**, 12821

Received 16th August 2020,
Accepted 17th September 2020

DOI: 10.1039/d0cc05578f

rsc.li/chemcomm

Reversible switching from a three- to a nine-fold degenerate dynamic slider-on-deck through catenation†

Vishnu Verman Rajasekaran, Indrajit Paul and Michael Schmittel *

Two dynamic slider-on-deck assemblies, *i.e.* a two-component threefold degenerate (k_{298} = 34.9 kHz) and a catenated three-component ninefold degenerate (k_{298} = 27.9 kHz) system, were quantitatively interconverted. Inspection of their computed structures revealed an allosteric effect on the sliding rates due to the spatial interaction between the components.

Since the first breathtaking demonstration of their preparation by simple self-assembly, catenanes[1] have assumed an outstanding importance in the arena of synthetic molecular machines.[2–4] These mechanically interlocked molecules have been the basis for constructing motors,[5] switches,[6] solid-state electronics,[7] and DNA-based architectures[8] mainly capitalizing on the relative translational and/or rotational dynamics between the rings. The inherent dynamics has been studied in much detail, as reported initially in Sauvage's ground-breaking [2]catenane paper,[9] followed by many studies on electrochemically,[10] light-,[11] and chemically[12] induced motion.[13]

To date, a lot of impressive examples of coordination-driven multicomponent dynamic catenanes have been reported,[14] but dynamics has been usually limited to the relative motion between rings.[15] In contrast, the concept of a multicomponent dynamic catenate exhibiting nanomechanical motion other than dynamics between rings has been a relatively unexplored facet.[16] Moreover, to the best of our knowledge, the allosteric adjustment of nanomechanical motion in multicomponent[17] dynamic catenanes adds new prospects for the field of catenate-based machines.

In this report, we elaborate on aspects of dual dynamics in catenate **DS2**, with the interconversion between topological structures (catenate → 2 × macrocycles) being only one facet (Scheme 1). A similar system developed by Sauvage and Heitz on the basis of homoleptic $[Cu(phen)_2]^+$ and N_{py} → ZnPor (zinc porphyrin) interactions, has emphasized the effect of geometric parameters (distance and angles) in coordination-based catenate assemblies.[18] The second facet of dynamics encompasses the feature that each macrocyclic unit of catenate **DS2** and of **DS1** is a highly dynamic slider-on-deck system in itself (*e.g.* **DS1**, Scheme 1). In more detail, the dynamic two-component slider-on-deck **DS1** constitutes a macrocyclic system with three degenerate states that reversibly and quantitatively converts into the three-component dynamic slider-on-deck catenate **DS2** with 3 × 3 degenerate states. Interconversion is accomplished by addition/removal of Cu^+ ions. Moreover, the intrasupramolecular dynamics, the rate-determining step of which requires N_{py} → ZnPor bond cleavage, is affected by an allosteric effect originating at the remote metal-phenanthroline coordination site.

Synthesis and characterization of biped **1** and deck **2** are described in the ESI.† At first, we decided to separately prepare the multicomponent dynamic slider-on-deck systems **DS1** and **DS2** capitalizing on homoleptic $[Cu(phenAr_2)_2]^+$ complexation and/or N_{py} → ZnPor interactions, *i.e.* two binding motifs that are known to be orthogonal.[19] Biped **1** and deck **2** were mixed

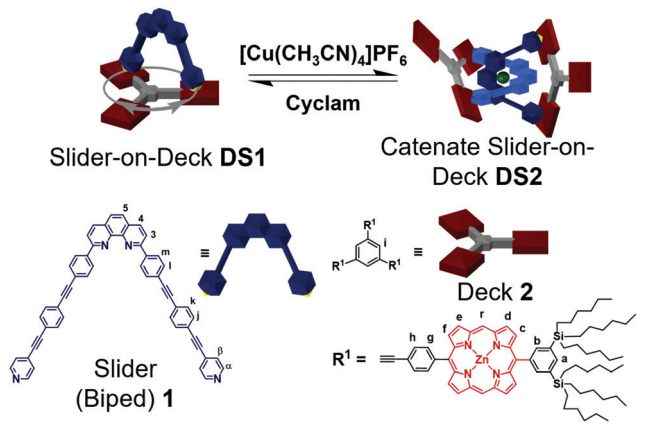

Scheme 1 Reversible interconversion between the slider-on-deck **DS1** and the dynamic catenate slider **DS2**. Sliding motion shown for **DS1**.

Center of Micro and Nanochemistry and Engineering, Organische Chemie I, Universität Siegen, Adolf-Reichwein-Str. 2, D-57068, Germany.
E-mail: schmittel@chemie.uni-siegen.de; Tel: +49(0) 2717404356

† Electronic supplementary information (ESI) available. See DOI: 10.1039/d0cc05578f

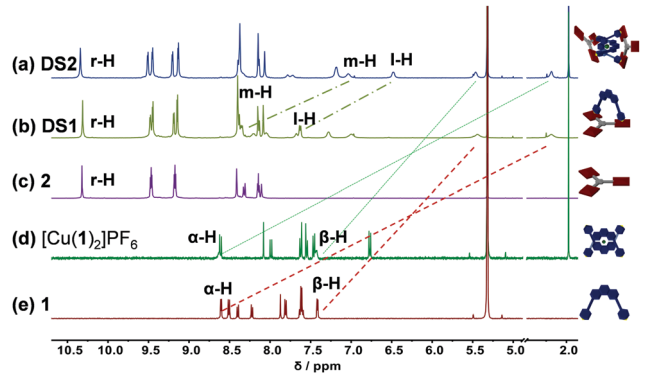

Fig. 1 Comparison of partial ^{1}H-NMR (500 MHz, CD_2Cl_2, 298 K) of (a) catenate slider-on-deck **DS2** = $[Cu(\mathbf{1})_2{\cdot}(\mathbf{2})_2]PF_6$; (b) slider-on-deck **DS1** = [**1**·**2**]; (c) free deck **2**; (d) $[Cu(\mathbf{1})_2]PF_6$; (e) slider **1**.

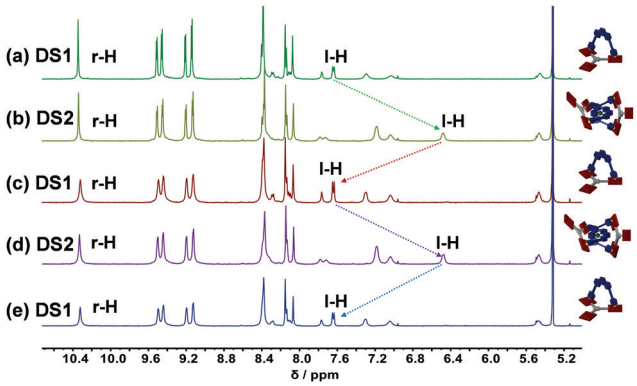

Fig. 2 Partial ^{1}H-NMR (500 MHz, CD_2Cl_2, 298 K) of the reversible interconversion between slider-on-deck **DS1** to catenate slider-on-deck **DS2** over 2.5 cycles. The quantitative catenation/decatenation was followed by monitoring the drastically different ^{1}H-NMR signal of proton l-H. (a) Mixing ligands **1** and **2** in 1 : 1 ratio furnished **DS1**. (b) Addition of 0.5 equiv. of Cu^+ furnished **DS2** (catenation). (c) Addition of 0.5 equiv. of cyclam and sonication of the mixture at 50 °C for 30 min afforded **DS1** (de-catenation). (d) Addition of 0.5 equiv. of Cu^+ resulted in quantitative formation of **DS2** (catenation). (e) Subsequent addition of cyclam followed by sonicating the mixture at 50 °C for 30 min furnished **DS1** as a clean assembly (de-catenation).

in a 1 : 1 ratio quantitatively furnishing **DS1** (Fig. 1b). Complex **DS1** was fully characterized by ^{1}H, ^{1}H–^{1}H COSY, ^{1}H–^{1}H NOESY, ^{1}H DOSY NMR studies and elemental analysis (ESI,† Fig. S17–S19, S25). The slider assembly was identified by the changes in the ^{1}H-NMR signals of protons α-H, β-H of the biped **1** and r-H of the deck **2** (Fig. 1b, c and e). There are stark changes in the signals of protons α-H and β-H of **1** as they experience the porphyrin's shielding ring current upon axial N_{py} → ZnPor coordination thus shifting the r-H signals of **2** slightly upfield.

Similarly, **1**, **2** and Cu^+ were mixed in a 2 : 2 : 1 ratio to quantitatively assemble **DS2**. The complex **DS2** was fully characterized by ^{1}H NMR, ^{1}H–^{1}H COSY, ^{1}H–^{1}H NOESY NMR, ^{1}H DOSY (ESI,† Fig. S20–S22, S24), and elemental analysis. Formation of the dynamic catenate **DS2** was ascertained by changes in the ^{1}H-NMR signature of protons m-H, l-H, α-H, β-H of **1** and r-H of **2**. Signals of protons α-H and β-H significantly shifted upfield, while those of m-H and l-H from the $[Cu(\mathbf{1})_2]^+$ unit broadened and shifted slightly upfield upon catenation and axial coordination with **2** (Fig. 1a and d). The broadening is a strong indication of dynamic exchange rates faster than the NMR timescale.

Finally, we were interested in reversibly interconverting the two slider-on-deck systems and thus first assembled **DS1** in solution as described above. Follow-up addition of 0.5 equiv. of $[Cu(CH_3CN)_4]PF_6$ quantitatively furnished **DS2**. Sequential addition and removal of Cu^+ (using cyclam followed by sonication at 50 °C for 30 min) led to quantitative interconversion between the two assemblies **DS1** and **DS2** (Fig. 2a–e). The transformation **DS1** → **DS2** was confirmed by drastic upfield shifts of the ^{1}H-NMR signals of protons m-H and l-H attributed to the shielding by the proximal second phenanthroline. These findings were further corroborated by ^{1}H-DOSY NMR studies (ESI,† Fig. S24 and S25) which indicated a hydrodynamic radius change proportionate to the larger catenate slider-on-deck **DS2** ($D = 3.30 \times 10^{-10}$ m^2 s^{-1}, $r_s = 16.1$ Å) when compared to **DS1** ($D = 3.82 \times 10^{-10}$ m^2 s^{-1}, $r_s = 13.9$ Å).

To quantify the sliding exchange dynamics, we analyzed the ^{1}H-NMR signals of **DS1** at various temperatures. The diagnostic proton r-H signal of the ZnPor units in **DS1** was chosen because it appears as a sharp singlet (10.34 ppm) at 298 K. VT ^{1}H-NMR studies[20] confirmed the dynamic coordination of both pyridine terminals of the slider biped **1** to the three degenerate ZnPor stations of deck **2**. Diagnostically, the sharp singlet at 298 K separated at 228 K into two singlets (2 : 1) at 10.32 and 10.40 ppm. While the rather sharp signal at 10.32 ppm was assigned to both pyridine-coordinated zinc porphyrins, the freely rotating second zinc porphyrin furnished a broader signal at 10.40 ppm. A kinetic analysis provided the frequency (k) for exchange at different temperatures (Fig. 3a) with k = 34.9 kHz s^{-1} at 298 K. The activation parameters are $\Delta H^{\ddagger}$ = 52.2 ± 0.7 kJ mol^{-1} and $\Delta S^{\ddagger}$ = 17.2 ± 2.8 J mol^{-1} K^{-1} furnishing the free energy of activation for exchange at 298 K as $\Delta G^{\ddagger}_{298} = 47.1 \pm 0.1$ kJ mol^{-1} (ESI,† Fig. S28 and S29).

Analogously, the proton r-H signal was chosen as the diagnostic parameter in the VT ^{1}H-NMR for determining the dynamics of the catenate slider-on-deck **DS2**. At 298 K, the r-H signal showed up as a sharp singlet (10.34 ppm). The VT ^{1}H-NMR data thus confirmed the dynamic coordination of the tetratopic $[Cu(\mathbf{1})_2]PF_6$ with its four

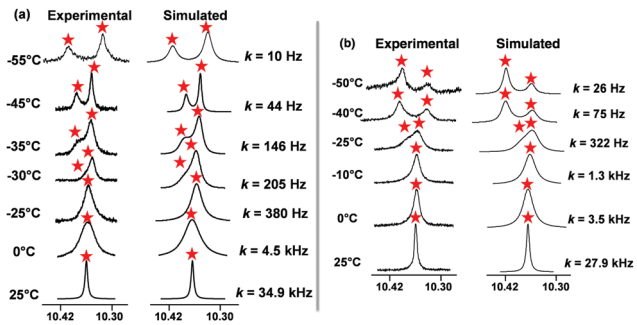

Fig. 3 The ^{1}H-VT-NMR (600 MHz) was undertaken for both systems in CD_2Cl_2. Experimental and theoretical splitting of the proton signal of (a) r-H in the slider-on-deck **DS1**, (b) r-H in the catenate slider-on-deck **DS2**.

pyridine terminals to the altogether 2 × 3 degenerate porphyrins from both identical decks **2**. At 233 K, the sharp singlet of proton r-H at 298 K separated into two singlets (2 : 1) at 10.40 and 10.32 ppm. Whereas the quite sharp signal at 10.40 ppm was ascribed to the four pyridine-coordinated zinc porphyrins, the two freely rotating zinc porphyrin(s) displayed a broader signal at 10.32 ppm. A kinetic analysis provided the frequency (k) for exchange at different temperatures (Fig. 3b) with k_{298} = 27.9 kHz at 298 K. The activation parameters are $\Delta H^{\ddagger}$ = 48.9 ± 0.7 kJ mol^{-1} and $\Delta S^{\ddagger}$ = 3.2 ± 2.6 J mol^{-1} K^{-1} furnishing the free energy of activation for exchange at 298 K as $\Delta G^{\ddagger}$ = 47.9 ± 0.1 kJ mol^{-1} (ESI,† Fig. S26 and S27).

For similar slider-on-deck systems,[21,22] we recently discussed various mechanistic options, but only one scenario agreed with the kinetic data. Alike, in both **DS1** and **DS2** the exchange could occur through complete dissociation followed by re-association of **1** and **2** (intermolecular hopping) or a single N_{py} → ZnPor bond dissociation-rotation-association (sliding) mechanism. Since the barrier in a rotor[23] operating *via* a well-defined single N_{py} → ZnPor dissociation amounted to $\Delta G^{\ddagger}$ = 47.6 ± 0.1 kJ mol^{-1}, the pathway involving complete dissociation is rigorously ruled out for **DS1** and **DS2** as their barriers are almost identical to that of the rotor: $\Delta G^{\ddagger}$ (**DS1**) = 47.1 ± 0.1 kJ mol^{-1} and $\Delta G^{\ddagger}$ (**DS2**) = 47.9 ± 0.1 kJ mol^{-1}.

Comparing the kinetic data of both slider-on-deck systems leads us to interesting mechanistic corollaries. Specifically, one could hypothesize that the exchange motion at both ZnPor decks of **DS2** could be either coupled or decoupled. If the exchange would be decoupled, *i.e.* the motion at both decks is fully independent, then the frequency should be identical to that of **DS1**. If it were coupled, positions at deck A and B would communicate and then a full exchange would require that all combinations be passed through equally. As a result, the frequency could be derived from the exchange rate at the single site in **DS1** and a statistical correction. In principle, this constitutes a case of multiplicative constrained probabilities as $P_{(\text{total})} = P_{(\text{event 1})} \times P_{(\text{event 2; given event 1 has happened})}$. In the coupled case one would expect $P_{(\text{total})}$ = (1/3) × (1) = 1/3. However, the observed rate of **DS2** is not 1/3 that of **DS1**; the frequency at **DS2** is only slower by 10–15%. On the other hand, the two rates are not identical, as expected for the decoupled case. Rather they remain different even considering the error range (k_{298} = 34.9 ± 1.8 kHz for **DS1** and k_{298} = 27.9 ± 1.4 kHz for **DS2**). Nevertheless, it is obvious to postulate for **DS2** that the motion at both decks is decoupled. But why is the observed frequency lower? We can exclude metal coordination at the remote phenanthroline to be responsible for this effect. Actually, metal coordination should lower the donor quality of the pyridine feet in the N_{py} → ZnPor interaction. As a net effect, in such case, exchange in **DS2** should be faster than in **DS1**, contrary to our findings.

Ultimately, an inspection of the DFT-computed slider-on-deck structures provides a convincing reason for the rate differences. The data suggest that biped **1** in **DS1** (ESI,† Fig. S35) is strained once axial N_{py} → ZnPor coordination at both ZnPor units is realized. The strain is indirectly visible from the intramolecular pyridine–pyridine distance when one compares the

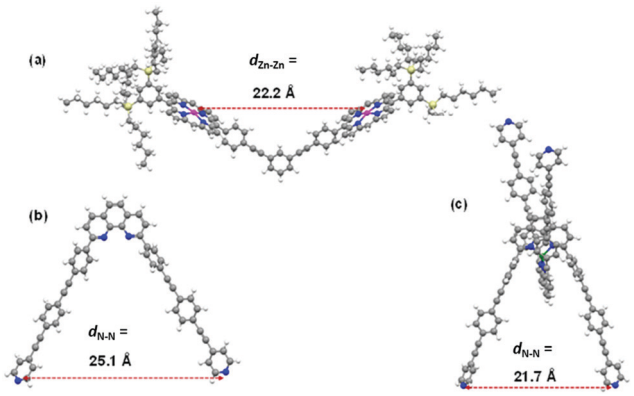

Fig. 4 Ball and stick representation of (a) partial structure of deck **2**. (b) Structure of biped **1**. (c) Structure of [Cu(**1**)$_2$]$^+$. All figures show the energy-minimized structures (B3LYP/6-31G(d); Lanl2dz basis set for metals). Counter anions are not included.

$d(N_{py}\text{–}N_{py}')$ of the free biped **1** in its unstrained state with the one enforced for **1** when combining with deck **2** in **DS1**, *i.e.* 25.1 *vs.* 22.2 Å, respectively (Fig. 4a and b). Consequently, some release of strain energy is expected to promote the N_{py} → ZnPor dissociation step in **DS1**. On the other hand, the computed [Cu(**1**)$_2$]$^+$ fragment in **DS2** (ESI,† Fig. S36) has an intramolecular pyridine–pyridine distance $d(N_{py}\text{–}N'_{py})$ = 21.7 Å that almost exactly matches that of the unstrained free deck **2** {d(Zn–Zn) = 22.2 Å} (Fig. 4a and c) leading to a possibly strain-free axial N_{py} → ZnPor coordination in **DS2**. The reduced $N_{py}\text{–}N'_{py}$ distance in the [Cu(**1**)$_2$]$^+$ unit as compared to that in **1** indicates a long-range effect of the Cu$^+$ coordination on the biped's spatial arrangement. This finding points to an allosteric effect originating from the four-fold π–π stacking between the 2,9-phenyl groups with the opposite phenanthroline's π cloud in the homoleptic complex [Cu(**1**)$_2$]PF$_6$.

Finally, due to the reduced strain release in the transition state of the exchange in **DS2** as compared to that in **DS1**, the slower sliding speed of 27.9 ± 1.4 kHz in **DS2** is readily understood (*cf.* **DS1**, k = 34.9 ± 1.8 kHz).

In summary, we have demonstrated two dynamic slider-on-deck systems that are quantitatively and reversibly toggled through catenation/decatenation. The interconversion between the two-component macrocyclic and the three-component slider-on-deck catenate is accomplished by addition and removal of Cu$^+$ ions. A rigorous kinetic analysis of the three- *vs.* nine-fold degenerate rearrangement indicates that allosteric effects are switched off/on in the **DS1** ⇆ **DS2** transformation. The fine tuning of dynamic allosteric effects in switchable multicomponent assemblies opens new routes for the modulation of molecular machine processes.

We are indebted to the University of Siegen, Dr Thomas Paululat (Siegen) and the Deutsche Forschungsgemeinschaft (Schm 647/20-2) for continued support.

Conflicts of interest

There are no conflicts to declare.

Notes and references

1 S.-L. Huang, T. S. A. Hor and G.-X. Jin, *Coord. Chem. Rev.*, 2017, **333**, 1–26.
2 S. Erbas-Cakmak, D. A. Leigh, C. T. McTernan and A. L. Nussbaumer, *Chem. Rev.*, 2015, **115**, 10081–10206.
3 J.-P. Sauvage, *Angew. Chem., Int. Ed.*, 2017, **56**, 11080–11093.
4 J. F. Stoddart, *Angew. Chem., Int. Ed.*, 2017, **56**, 11094–11125.
5 M. R. Wilson, J. Solà, A. Carlone, S. M. Goldup, N. Lebrasseur and D. A. Leigh, *Nature*, 2016, **534**, 235–240.
6 S. Grunder, P. L. McGrier, A. C. Whalley, M. M. Boyle, C. Stern and J. F. Stoddart, *J. Am. Chem. Soc.*, 2013, **135**, 17691–17694.
7 C. P. Collier, G. Mattersteig, E. W. Wong, Y. Luo, K. Beverly, J. Sampaio, F. M. Raymo, J. F. Stoddart and J. R. Heath, *Science*, 2000, **289**, 1172–1175.
8 (*a*) Y. Liu, A. Kuzuya, R. Sha, J. Guillaume, R. Wang, J. W. Canary and N. C. Seeman, *J. Am. Chem. Soc.*, 2008, **130**, 10882–10883; (*b*) J. Elbaz, Z.-G. Wang, F. Wang and I. Willner, *Angew. Chem., Int. Ed.*, 2012, **51**, 2349–2353.
9 M. Cesario, C. O. Dietrich-Buchecker, J. Guilhem, C. Pascard and J. P. Sauvage, *J. Chem. Soc., Chem. Commun.*, 1985, 244–247.
10 B. Korybut-Daszkiewicz, A. Więckowska, R. Bilewicz, S. Domagała and K. Woźniak, *Angew. Chem., Int. Ed.*, 2004, **43**, 1668–1672.
11 P. Mobian, J.-M. Kern and J.-P. Sauvage, *Angew. Chem., Int. Ed.*, 2004, **43**, 2392–2395.
12 N. H. Evans, C. J. Serpell and P. D. Beer, *Chem. – Eur. J.*, 2011, **17**, 7734–7738.
13 A. Goswami and M. Schmittel, *Coord. Chem. Rev.*, 2018, **376**, 478–505.
14 (*a*) M. Fujita and K. Ogura, *Coord. Chem. Rev.*, 1996, **148**, 249–264; (*b*) C. Dietrich-Buchecker, B. Colasson, M. Fujita, A. Hori, N. Geum, S. Sakamoto, K. Yamaguchi and J.-P. Sauvage, *J. Am. Chem. Soc.*, 2003, **125**, 5717–5725; (*c*) S. Prusty, S. Krishnaswamy, S. Bandi, B. Chandrika, J. Luo, J. S. McIndoe, G. S. Hanan and D. K. Chand, *Chem. – Eur. J.*, 2015, **21**, 15174–15187; (*d*) T. Sawada, M. Yamagami, K. Ohara, K. Yamaguchi and M. Fujita, *Angew. Chem., Int. Ed.*, 2016, **55**, 4519–4522.
15 N. H. Evans and P. D. Beer, *Chem. Soc. Rev.*, 2014, **43**, 4658–4683.
16 J. Valero, N. Pal, S. Dhakal, N. G. Walter and M. Famulok, *Nat. Nanotechnol.*, 2018, **13**, 496–503.
17 A. Goswami, S. Saha, P. K. Biswas and M. Schmittel, *Chem. Rev.*, 2020, **120**, 125–199.
18 M. Beyler, V. Heitz and J.-P. Sauvage, *J. Am. Chem. Soc.*, 2010, **132**, 4409–4417.
19 (*a*) N. Mittal, M. L. Saha and M. Schmittel, *Chem. Commun.*, 2015, **51**, 15514–15517; (*b*) S. De, S. Pramanik and M. Schmittel, *Angew. Chem., Int. Ed.*, 2014, **53**, 14255–14259.
20 (*a*) A. Goswami and M. Schmittel, *Angew. Chem., Int. Ed.*, 2020, **59**, 12362–12366; (*b*) S. Saha, P. K. Biswas, I. Paul and M. Schmittel, *Chem. Commun.*, 2019, **55**, 14733–14736; (*c*) A. Goswami, S. Pramanik and M. Schmittel, *Chem. Commun.*, 2018, **54**, 3955–3958.
21 I. Paul, A. Goswami, N. Mittal and M. Schmittel, *Angew. Chem., Int. Ed.*, 2018, **57**, 354–358.
22 A. Ghosh, I. Paul, S. Saha, T. Paululat and M. Schmittel, *Org. Lett.*, 2018, **20**, 7973–7976.
23 A. Goswami, I. Paul and M. Schmittel, *Chem. Commun.*, 2017, **53**, 5186–5189.